Differential Thermal Regimes of the Tarim and Sichuan Basins in China: Implications for Hydrocarbon Generation and Conservation

1922—2022

CHANG Jian[1, 2, *], LI Dan[1, 2], QIU Nansheng[1, 2], ZHU Chuanqing[1, 2], ZHONG Ningning[1, 2], FENG Qianqian[1, 2], ZHANG Haizu[3] and WANG Xiang[3]

[1] *State Key Laboratory of Petroleum Resources and Prospecting, China University of Petroleum, Beijing 102249, China*
[2] *College of Geosciences, China University of Petroleum, Beijing 102249, China*
[3] *Research Institute of Exploration and Development, Petro China Tarim Oilfield Company, Korla 841000, China*

Abstract: The uncertainty surrounding the thermal regimes of the ultra-deep strata in the Tarim and Sichuan basins, China, is unfavorable for further hydrocarbon exploration. This study summarizes and contrasts the present-day and paleo heat flow, geothermal gradient and deep formation temperatures of the Tarim and Sichuan basins. The average heat flow of the Tarim and Sichuan basins are 42.5 ± 7.6 mW/m^2 and 53.8 ± 7.6 mW/m^2, respectively, reflecting the characteristics of 'cold' and 'warm' basins. The geothermal gradient with unified depths of 0–5,000 m, 0–6,000 m and 0–7,000 m in the Tarim Basin are 21.6 ± 2.9 °C/km, 20.5 ± 2.8 °C/km and 19.6 ± 2.8 °C/km, respectively, while the geothermal gradient with unified depths of 0–5,000 m, 0–6,000m and 0–7,000 m in the Sichuan Basin are 21.9 ± 2.3 °C/km, 22.1 ± 2.5 °C/km and 23.3 ± 2.4 °C/km, respectively. The differential change of the geothermal gradient between the Tarim and Sichuan basins with depth probably results from the rock thermal conductivity and heat production rate. The formation temperatures at depths of 6,000 m, 7,000 m, 8,000 m, 9,000 m and 10,000 m in the Tarim Basin are 80°C–190°C, 90°C–220°C, 100°C–230°C, 110°C–240°C and 120°C–250°C, respectively, while the formation temperatures at depths of 6,000 m, 7,000 m, 8,000 m and 9,000 m in the Sichuan Basin are 120°C–200°C, 140°C–210°C, 160°C–260°C and 180°C–280°C, respectively. The horizontal distribution pattern of the ultra-deep formation temperatures in the Tarim and Sichuan basins is mainly affected by the basement relief, fault activity and hydrothermal upwelling. The thermal modeling revealed that the paleo-heat flow in the interior of the Tarim Basin decreased since the early Cambrian with an early Permian abrupt peak, while that in the Sichuan Basin experienced three stages of steady state from Cambrian to early Permian, rapidly rising at the end of the early Permian and declining since the late Permian. The thermal regime of the Sichuan Basin was always higher than that of the Tarim Basin, which results in differential oil and gas generation and conservation in the ultra-deep ancient strata. This study not only promotes theoretical development in the exploration of ultra-deep geothermal fields, but also plays an important role in determining the maturation phase of the ultra-deep source rocks and the occurrence state of hydrocarbons in the Tarim and Sichuan basins.

Key words: ultra-deep strata, heat flow, geothermal gradient, formation temperature, hydrocarbon generation and conservation, Sichuan Basin, Tarim Basin

Citation: Chang et al., 2022. Differential Thermal Regimes of the Tarim and Sichuan Basins in China: Implications for Hydrocarbon Generation and Conservation. Acta Geologica Sinica (English Edition), 96(4): 1308–1322. DOI: 10.1111/1755-6724.14980

1 Introduction

The ultra-deep strata below ~6,000 m in sedimentary basins have become the most important driver for hydrocarbon exploration and development in China, in the context of the increasing energy demand and the decrease in recovery for shallow oil and gas fields (Jin, 2011; Zou et al., 2018). In recent years, some giant oil and gas fields, such as the Shunbei oil field in the Tarim Basin and the Anyue gas field in the Sichuan Basin, were discovered (Wang et al., 2014; Zou et al., 2014; Jiao, 2018). It is noteworthy that the ultra-deep Cambrian and Ordovician reservoirs in the Tarim Basin still develop liquid hydrocarbon, while the ultra-deep Sinian and Cambrian reservoirs in the Sichuan Basin only retain gaseous hydrocarbon. Why are the oil and gas phases between these two basins for ultra-deep strata so different?

The formation temperature plays an essential role in hydrocarbon generation and conservation in petroliferous basins. Therefore, it is necessary to clarify the thermal regimes of the Tarim and Sichuan basins in order to resolve the above question. Previous studies have done some work on the present-day geothermal field and thermal history of these two basins (Li et al., 2010, 2022; Xu et al., 2011, 2018; Qiu et al., 2012, 2022; Liu et al., 2016, 2018, 2020; Chang et al., 2017a, 2022a, b; Zhu et al., 2022). However, there is no research to state the characteristics of the ultra-deep strata of the Tarim Basin

* Corresponding author. E-mail: changjian@cup.edu.cn

with depths of 6,000–10,000 m. In addition, the thermal regime comparison between the Tarim and Sichuan basins is somewhat involved. In this study, the present-day heat flow, geothermal gradients and ultra-deep formation temperatures of the Tarim are Sichuan basins are introduced and their differences further analyzed. The paleo-heat flow histories of the Tarim and Sichuan basins are then reconstructed based on the vitrinite reflectance data and basin modeling. Finally, the factors influencing the geothermal fields, source rock maturation evolution and differential oil and gas phases for the ultra-deep strata of the Tarim and Sichuan basins are discussed. This study provides new insights on the thermal regime of the Tarim and Sichuan basins, which will be of significance for further oil and gas exploration and resource evaluation of ultra-deep strata.

2 Geological Setting

This study involves the Tarim and Sichuan basins in China. As the largest basin in Central Asia with an area of 56 $\times 10^4$ km^2, the Tarim Basin lies in western China and is surrounded by South Tianshan to the north, the Kunlun Mountain to the southwest, the Altun Mountain to the southeast and the Kuluketage Mountain to the northeast (Fig. 1b). The Tarim Basin consists of nine tectonic units, including the Kalpin Uplift, Tabei Uplift, Central Uplift, Southeast Uplift, Kuqa Depression, Northern Depression, Southwest Depression, Tangguzibasi Depression and the Southeast Depression (Fig. 1b; Modified from Jia, 1997). The Central Uplift can be further divided into three secondary tectonic units, including the Guchengxu Uplift, Tazhong Uplift and Bachu Uplift. The Kongquehe Slope, Manjiaer Depression, Shuntuoguole Low-Uplift and Awati Depression belong to the secondary tectonic units of the Northern Depression.

The Tarim Basin developed on a Precambrian crystalline basement, covered by Paleozoic marine sediments and Mesozoic–Cenozoic terrestrial sediments (Zhang, 2000; He et al., 2005; Zhang et al., 2013). During the early Cambrian, the Tarim Basin was covered by seawater due to the global transgression, with thick dolomites deposited (Li et al., 2015; Yang et al., 2017). During the middle Cambrian, a suite of gypsum and salt rocks (of 0–450 m thickness) were deposited during the sea's retreat in the Shuntuoguole Low-Uplift, Awati Depression, Tazhong Uplift and Bachu Uplift (Yang, 2015). The eastern Tarim Basin predominantly deposited limestone and argillaceous limestone in the basin-slope facies environment from the Late Cambrian to the Middle Ordovician, while the western and central Tarim Basin deposited limestone, dolomites and slight reefs, which developed in the open to restricted platform environment. Lin et al. (2012) considered that the Tarim Basin mainly

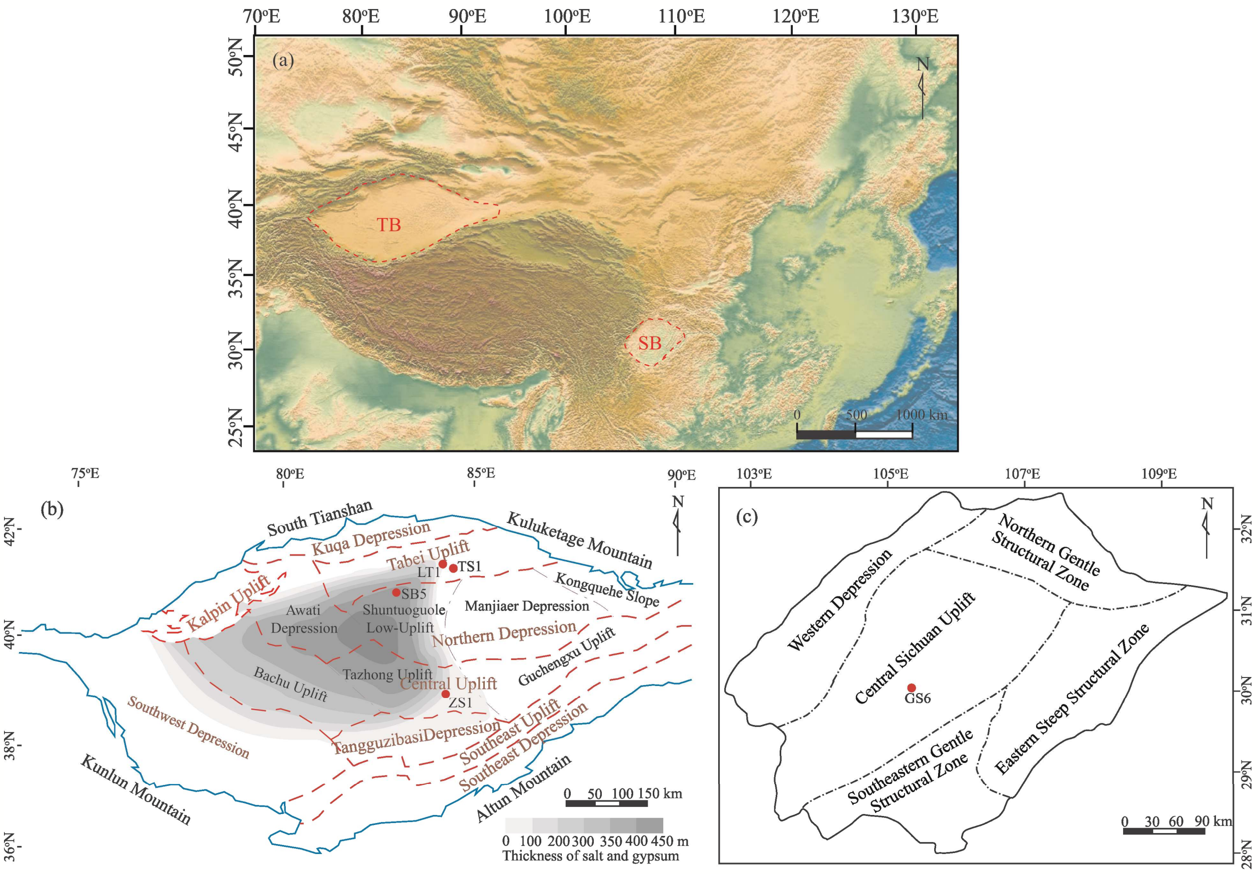

Fig. 1. (a) The locations of the Tarim and Sichuan basins in China. TB-Tarim Basin; SB-Sichuan Basin; (b) tectonic units in the Tarim Basin (Jia,1997), which indicate the distribution range of the salt and gypsum layer in the middle Cambrian (Yang, 2015) and the studied wells; (c) tectonic units in the Sichuan Basin (Qiu et al., 2022) and the studied wells.

deposited silicilastic rocks in the deep-sea environment during the Late Ordovician. Only the interior of the Tarim Basin deposited sandstones and mudstones within the environment of a coastal and shallow sea during the Silurian (Zhang et al., 2008; Chang et al., 2012). The neritic clastic rocks indicate that the Tarim Basin evolved as an epicontinental marine environment during the Carboniferous. The early Permian magmatic activity led the basalts, rhyolites and pyroclastic rocks to be deposited in the northwestern Tarim Basin (Li et al., 2011, 2012; Xu et al., 2014). Since the Triassic, the foreland basins began to develop in the northern and southwestern margins of the Tarim Basin, the Southwestern Depression, Kashi Depression and Kuqa Depression deposited clastic rocks with a thickness of several kilometers (Chang et al., 2017b). The superior marine source rocks in the Tarim Basin contain the Yuertusi Formation in the lower Cambrian and the Saergan Formation in the Middle Ordovician, which were characterized by the high total organic carbon (TOC) content (Yun et al., 2014). Exploration determined that the lower Cambrian dolomite under the middle Cambrian gypsum-salt layers and the carbonates of the Lower-Middle Ordovician Yijianfang-Yingshan formations, with faults and karst features, are the typical ultra-deep hydrocarbon reservoirs (Yun and Zhai, 2008; Jiao, 2018; Liu et al., 2021).

The Sichuan Basin is located on the western margin of the South China block and is characterized by a rhomboid shape with an area of ~1.9×10^5 km^2. It is bounded by the Songpan-Ganzi Fold belt and Longmen Mountain to the west, Micang and Daba Mountains to the north, Qiyue Mountain to the east, and Daliang and Dalou Mountains to the south. According to the tectonic, sedimentary and basement characteristics, the Sichuan Basin can be further divided into five sub-structural units: The Western Depression, Northern Gentle Structural Zone, Eastern Steep Structural Zone, Central Sichuan Uplift and Southeastern Gentle Structural Zone.

The Sichuan Basin, developed on the Upper Yangtze platform basement, experienced a Sinian–Middle Triassic cratonic depression stage and a Late Triassic–Quaternary foreland basin stage (He et al., 2020; Liu et al., 2021; Yang et al., 2020). Correspondingly, the strata of the Sichuan Basin, with a total thickness of 5–10 km, consists of two sedimentary systems, including the lower marine carbonate sedimentary system and the upper continental clastic sedimentary system (Xu et al., 2018). As a result of the multiple tectonic movements, the Sichuan Basin primarily developed four unconformities, which can be found in the interfaces of the upper Sinian and the lower Cambrian, the Permian and the underlying strata, the Middle Triassic and the Upper Triassic, as well as the Paleogene and the underlying strata, (Xu et al., 2018). The Qiongzhusi Formation black mudstone and shale of the lower Cambrian in the Central Sichuan Uplift are good source rocks, with type I marine organic matter and a TOC content of 0.5%–1.4% (Zou et al., 2014; Zhou et al., 2015). The lower Cambrian Longwangmiao Formation and the second member of the Sinian Dengying Formation (Z_2dn^2) are the reservoirs, in which the Anyue giant gas field, with a proved reserve of 4.4 $\times 10^{11}$ m^3, was discovered.

3 Present-day Geothermal Field of the Tarim and Sichuan Basins

3.1 Heat flow

The surface heat flow provides important heat information for the interior of the earth. It is equal to the geothermal gradient multiplied by rock thermal conductivity. According to the massive heat flow data, Qiu et al. (2022) conducted a systematic analysis on the horizontal distribution characteristics of the present-day heat flow in the Tarim and Sichuan basins (Fig. 2). The heat flow of the Tarim Basin ranges from 27.4 mW/m^2 to 66.5 mW/m^2, with an average value of 42.5 ± 7.6 mW/m^2 (Fig. 2a), indicating that the Tarim Basin is a typical ‘cold’ basin. Generally, the uplifted areas with a shallow basement show higher heat flow (such as southeast Tarim Basin, with heat flow over 60 mW/m^2), while the heat flow value in the depression areas with thick Cenozoic sediments including the Southwest Depression and Northern Depression is relatively low, with the values lying between 30–40 mW/m^2. The abnormal high heat flow in the Kuqa Depression and the western margin of the Bachu Uplift probably resulted from thermal disturbance caused by thrust and strike-slip fault activity, respectively, during the late Cenozoic.

The average heat flow of the Sichuan Basin is 53.8 ± 7.6 mW/m^2 (Fig. 2b). The Central Sichuan Uplift and

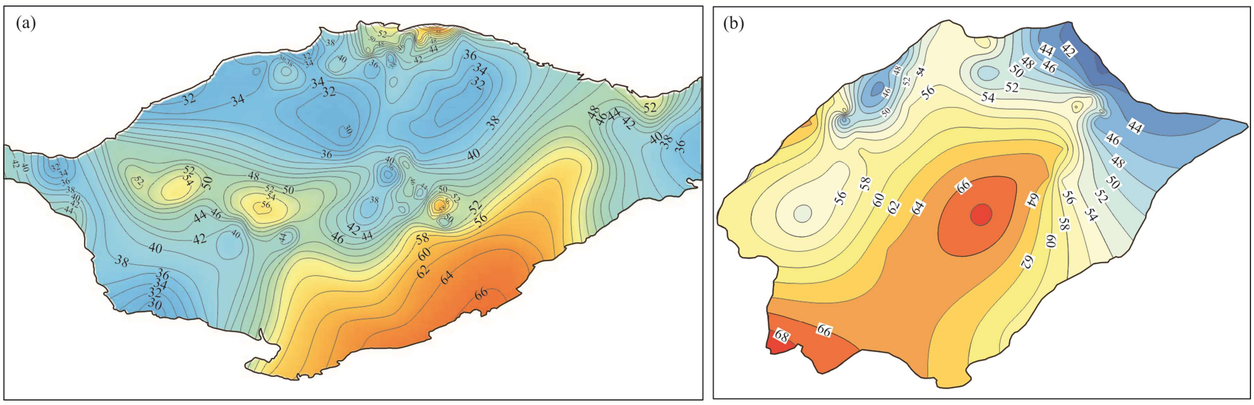

Fig. 2. Horizontal distribution characteristics of present-day heat flow in the Tarim and Sichuan basins (Qiu et al., 2022).

Southeastern Gentle Structural Zone display high heat flow, with a range of 60–70 mW/m^2, while the heat flow in the north-central part of the Western Depression, the Northern Gentle Structural Zone and the north of the Eastern Steep Structural Zone was very low, with 40–54 mW/m^2. Compared to the Tarim Basin, the Sichuan Basin shows much higher heat flow and is a typical 'warm' basin.

3.2 Geothermal gradient

The geothermal gradient is the amount that the formation temperature in the basins increases with burial depth. Previous studies confirmed that the geothermal gradient in the sedimentary basins varies with depth (Feng et al., 2009; Chang et al., 2016a; Liu et al., 2020; Zuo et al., 2020). Therefore, the geothermal gradient with unified depth can represent the actual thermal regime of the sedimentary basin (Chang et al., 2016a). Chang et al. (2016a) introduced the calculation method for the geothermal gradient of unified depth. Firstly, the formation temperatures at one unified depth for all the wells are calculated by 1D steady-state heat conduction equation, then the geothermal gradient is equal to the calculated formation temperature divided by the unified depth. Figure 3 indicates the horizontal distribution pattern of the geothermal gradient with the unified depths of 0–5,000 m, 0–6,000 m and 0–7,000 m for the Tarim Basin and with the unified depths of 0–5,000 m, 0–6,000 m and 0–8,000 m for the Sichuan Basin.

The geothermal gradient with a unified depth of 0–5,000 m in the Tarim Basin ranges from 14.9 °C/km to 31.9 °C/km with an average value of 21.6 ± 2.9 °C/km (Fig. 3a). The southeast Tarim Basin and the northern margin of the Kuqa Depression show the highest geothermal gradient with 28–30 °C/km, while the Kalpin Uplift has the lowest geothermal gradient with 12–16 °C/

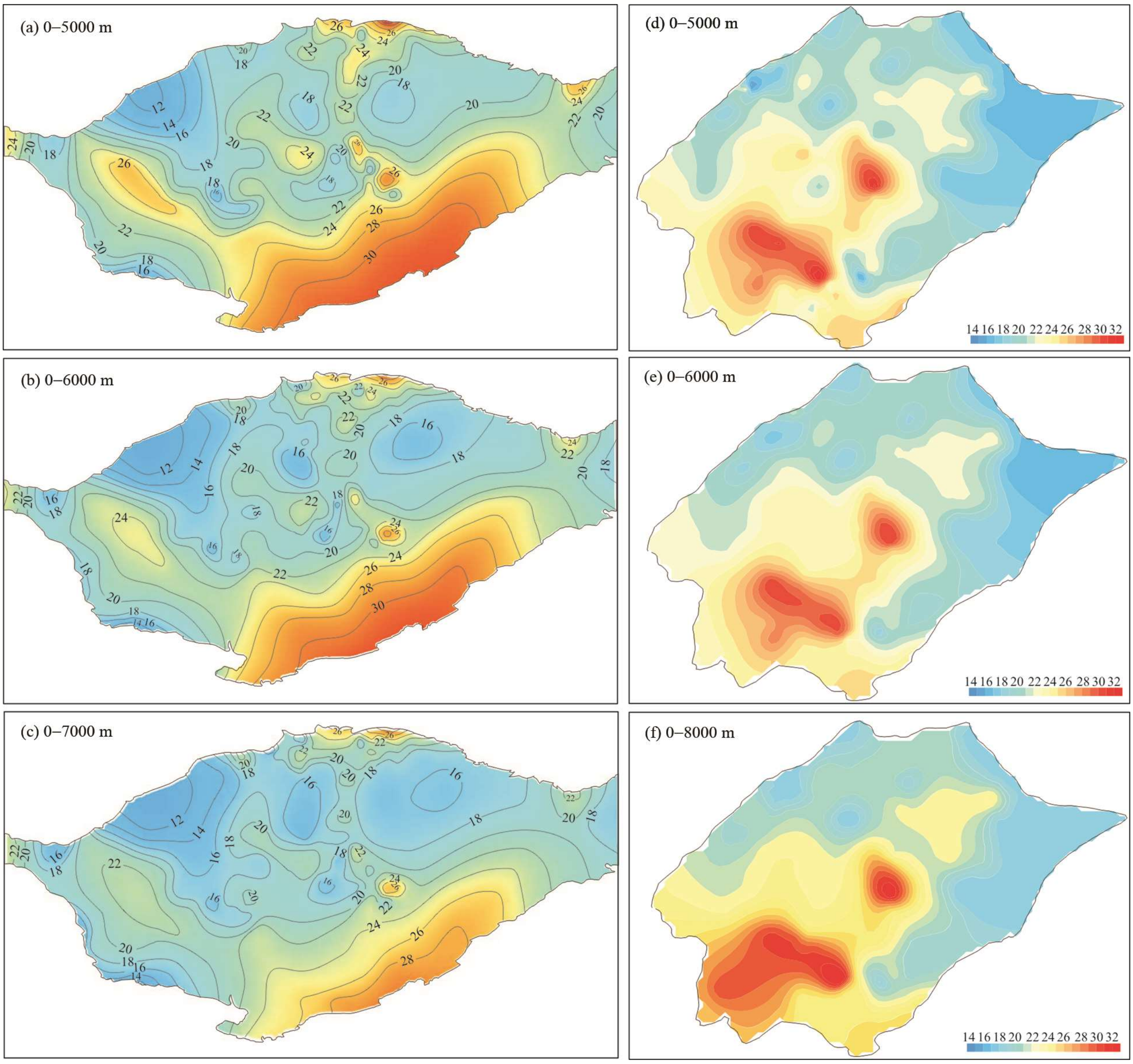

Fig. 3. Horizontal distribution of the geothermal gradient with different unified depths in the Tarim and Sichuan basins.

km. The geothermal gradient in the western margin of the Southwest Depression, northern Shuntuoguole Low-Uplift, Manjiaer Depression and Kongquehe Slope range from 16–20 °C/km. The eastern Southwest Depression and southern Shuntuoguole Low-Uplift show relatively high geothermal gradients with 22–26 °C/km, which is related to the deeper hydrothermal upwelling (Liu et al., 2020). The average geothermal gradients with unified depths of 0 –6,000 m and 0–7,000 m in the Tarim Basin are 20.5 ± 2.8 °C/km (14.0–31.7 °C/km) and 19.6 ± 2.8 °C/km (13.3–31.4° C/km) (Fig. 3b–c). Their horizontal distribution characteristics resemble the unified depth of 0-5,000m, but the geothermal gradients decrease with increasing depth.

The geothermal gradient with a unified depth of 0–5,000 m in the Sichuan Basin ranges from 14.8 °C/km to 30.3 °C/km, with an average value of 21.9 ± 2.3 °C/km (Fig. 3d). Generally, the geothermal gradient in the Sichuan Basin increases from north to south. The geothermal gradient of the Central Sichuan Uplift and the Southeastern Gentle Structural Zone ranges from 22–32 °C/km and is higher than that of the Northern Gentle Structural Zone, Western Depression and Eastern Steep Structural Zone with the value of 14–20°C/km. The average geothermal gradients with the unified depths of 0–6,000 m and 0–8,000 m in the Sichuan Basin are 22.1 ± 2.5 °C/km (16.1–31.0 °C/km and 23.3 ± 2.4°C/km (18.0–33.6 °C/km) (Fig. 3e–f), indicating that the geothermal gradient in the Sichuan Basin increases with increasing depth, which is different from the Tarim Basin.

3.3 Deep temperatures

The breakthrough in oil and gas exploration beneath the depth of ~6,000 m indicated that it is necessary to clarify the ultra-deep formation temperatures of the Tarim and Sichuan basins for better evaluation of the current ultra-deep hydrocarbon generation and conservation abilities (Yun and Zhai, 2008; Wang et al., 2014; Jiao, 2018). As the geothermal gradient of the basins usually varies with depth, the ultra-deep formation temperature obtained from multiplying the shallow geothermal gradient by the depth would not be the actual geological condition (Liu et al., 2020). In this study, the one-dimensional steady-state heat

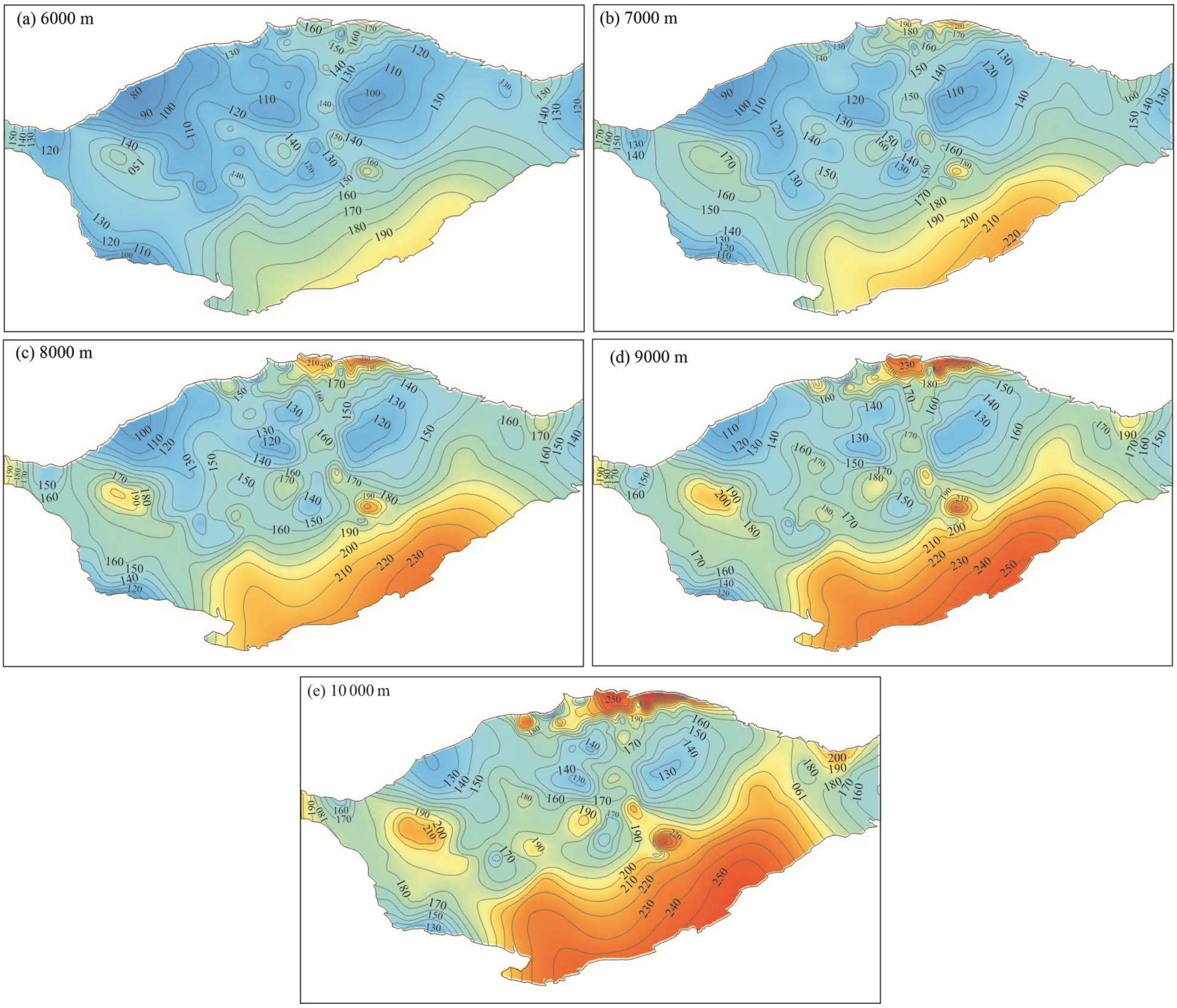

Fig. 4. Horizontal distribution pattern of the formation temperature at depths of 6,000 m, 7,000 m, 8,000 m, 9,000 m and 10,000 m in the Tarim Basin.

conduction equation (1) was adopted to calculate the ultra-deep formation temperature of the Tarim and Sichuan basins. Equation (2) is used to calculate the heat flow of the i+1 layer.

$$T_{i+1} = T_i + \frac{q_i}{K_i}\Delta z_i - \frac{A_i \cdot \Delta z_i^2}{2K_i} \quad (1)$$

$$qi_{+1} = q_i - A_i \cdot \Delta z_i \quad (2)$$

where A_i, K_i, and Δ_{Zi} are the heat production rate ($\mu W/m^3$), thermal conductivity (W/(m K)) and the thickness of the i_{th} layer, respectively; T_i and T_{i+1} are the temperatures at the top and bottom of the i_{th} layer, respectively; q_i and q_{i+1} are the heat flow at the top and bottom of the i_{th} layer, respectively. T_0 is the present-day surface temperature, 14°C; q_0 is the surface heat flow (Fig. 2). The heat production rate and thermal conductivity of each stratum (layer) refers to the data of Liu et al. (2016) and Zhu et al. (2022). The thickness of each stratum (layer) was obtained from the drilling and/or seismic data. The distribution characteristics of the calculated ultra-deep temperatures at depths of 6,000–10,000 m for the Tarim Basin and 6,000–9,000 m for the Sichuan Basin are shown in Figs. 4 and 5, respectively.

For the Tarim Basin, the formation temperatures of the Tarim Basin at a depth of 6,000 m range from 80°C to 190°C (Fig. 4a). The southeast Tarim Basin and northern Kuqa Depression display relatively higher temperatures with 160–190°C, while the formation temperatures of the Kalpin Uplift are less than ~110°C. Most of the Bachu Uplift, Tazhong Uplift, Northern Depression and the western Southwest Depression have temperatures of 100–130° C. The formation temperatures in the Kuqa Depression and Tabei Uplift decrease from ~180°C in the north to ~120°C in the south. For the depth of 7,000 m, the formation temperature ranges from 110°C to 220°C (Fig. 4b). The southwest Tarim Basin and northern Kuqa Depression show higher formation temperatures, more than ~180°C, while the Kalpin Uplift shows the lowest temperature of 90–120°C. The formation temperatures of the remaining areas in the Tarim Basin are predominantly distributed between 120–150° C. The formation temperatures of the depths 8,000 m, 9,000 m and 10,000 m increase from 100–230°C to 120–250°C (Fig. 4c–e), indicating similar distribution characteristics to that of the 6,000 m and 7,000 m depths. Moreover, the comparison between the measured and calculated temperature data for some typical wells indicates that the horizontal distribution pattern of the formation temperatures at depths of 6,000–10,000 m in the Tarim Basin is reliable (Table 1). It is worth noting that the formation temperature

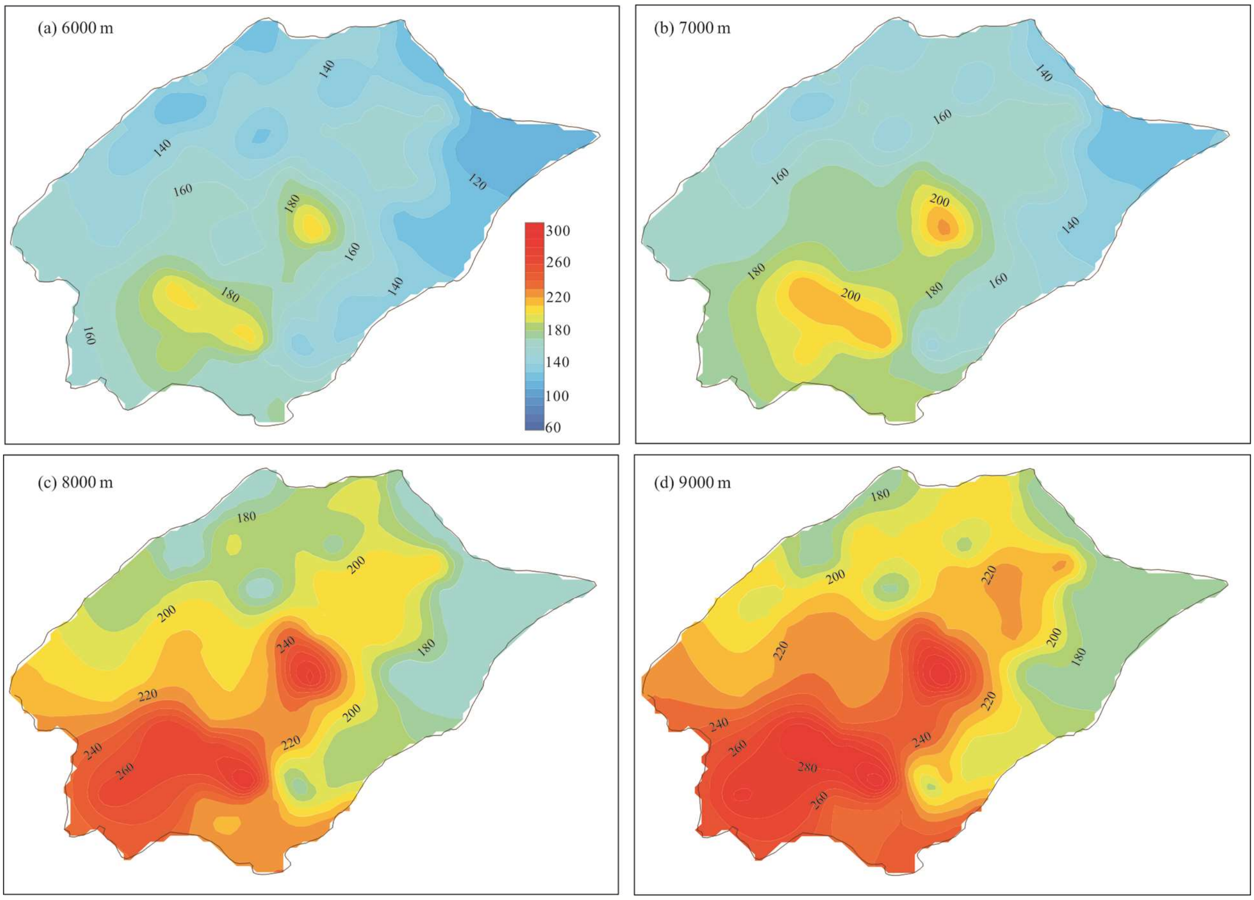

Fig. 5. Horizontal distribution pattern of the formation temperature at depths of 6,000 m, 7,000 m, 8,000 m and 9,000 m in the Sichuan Basin (Modified from Zhu et al., 2022).

Table 1 Comparison between measured and calculated temperature data for some typical wells in the Tarim Basin

Well name	Depth and measured temperature	Depth and calculated temperature
QG2	6125 m (157.0°C)	6000 m (155.0°C)
MX2	6200 m (129.0°C)	6000 m (127.0°C)
LT1	8200 m (160.4°C)	8000 m (158.0°C)
MS1	7514 m (157.1°C)	8000 m (162.0°C)

at a depth of 10,000 m in the northern Shuntuoguole Low-Uplift and Manjiaer Depression is just 130–170°C, which is suitable for liquid hydrocarbon conservation.

The formation temperature at a depth of 6,000 m in the Sichuan Basin ranges from 120–200°C (Fig. 5a). The Northern Gentle Structural Zone, Western Depression and Eastern Steep Structural Zone show relatively low formation temperatures of 120–150°C, while the formation temperature in the Central Sichuan Uplift and Southeastern Gentle Structural Zone is more than 160°C. The formation temperatures at the depths of 7,000 m, 8,000 m and 9,000 m increase from 140–210°C to 180–280°C (Fig. 5b–d), indicating a similar distribution to that of 6,000 m depth. The formation temperature at the depth of 9,000 m for most of the Sichuan Basin is higher than 180°C, which could result in crude oil cracking and is therefore unsuitable for liquid hydrocarbon conservation.

4 Paleo-heat Flow Histories of the Tarim and Sichuan Basins

The past thermal regime of sedimentary basins can be expressed by the paleo-heat flow and paleo-geothermal gradient (Qiu et al., 2012; Chang et al., 2016b, 2018), which play an important role in accurately revealing hydrocarbon generation and accumulation times. The joint vitrinite reflectance data (*R*o) and basin modeling are usually used to reconstruct the paleo-heat flow history of sedimentary basins (Chang et al., 2018; Fig. 6). In this study, the Basinmod 1D software was operated to model the heat flow histories of the Tarim Basin with the Easy%*R*o model (Sweeney and Burnham, 1990). First, the sedimentary and burial histories of the drillings were rebuilt, according to the borehole data, then constraints such as the vitrinite reflectance data and the present-day heat flow were input. Secondly, the paleo-heat flow paths used in the forward modeling were repeatedly changed and the correlation between the modeled *R*o paths and the measured *R*o data was analyzed. The corresponding paleo-heat flow path was considered to be the actual heat flow history when the modeled *R*o path overlapped with the measured *R*o data.

As the Cambrian and Ordovician source rocks and reservoirs were found in the interior of the Tarim Basin, this study mainly illustrates the paleo-heat flow histories of the Tazhong Uplift, Tabei Uplift and northern Shuntuoguole Low-Uplift (Fig. 7). Although the heat flow histories of the wells in each tectonic unit are different, the heat flow of these three tectonic units generally decreased since the early Cambrian. Due to the thermal effect of the large igneous province (LIP), there is an abrupt peak in the heat flow in the western Tabei Uplift, northwest Tazhong Uplift and northern Shuntuoguole Low-Uplift. In addition, the heat flow of the northern Shuntuoguole Low-Uplift was much lower than that of the Tabei Uplift and the Tazhong Uplift. This is because the northern Shuntuoguole Low-Uplift remained in a long-term stable state during the geological timescale.

The heat flow histories in the Sichuan Basin could be divided into three stages: a steady state before the early Permian, a rapid rising at the end of the early Permian and a decline after the late Permian (Fig. 8; Qiu et al., 2022). As the thermal effect generated by the Emeishan mantle plume gradually became weak from south to north in the Sichuan Basin, the peak value of the heat flow during the late Permian became smaller from southwest Sichuan to northeast Sichuan (Jiang et al., 2018; Qiu et al., 2022).

5 Discussion

5.1 Influence aspect for ultra-deep geothermal field variation

The variation of ultra-deep formation temperatures in sedimentary basins is usually related to basement relief, rock thermal conductivity, fault activity and/or hydrothermal upwelling. Most basins in the world are characterized by an obvious correspondence between the present-day geothermal gradient, heat flow and basement relief (Förster et al., 1997; Xu et al., 2011; Chang et al., 2016a; Liu et al., 2016; Putra et al., 2016; Poulsen et al., 2017; Majorowicz and Grasby, 2019). The geothermal gradient and heat flow in the uplift regions of the sedimentary basins are usually higher than that in the depression regions. This is because the bedrocks in the uplift regions usually show higher thermal conductivity than the sandstone and mudstone sediments deposited in the depression regions. The 'thermal refraction' effect caused by differential rock thermal conductivities finally led the heat energy in the sedimentary basins to accumulate in the uplift regions (Xiong and Gao, 1982; Chang et al., 2016a). Finally, the uplift regions of the sedimentary basins have a higher temperature zone than the depression regions (Fig. 9a). The horizontal distribution pattern of the present-day heat flow and deep formation temperatures in the Sichuan Basin is predominantly controlled by the basement relief (Xu et al., 2011; Zhu et al., 2022). Liu et al. (2016) considered that the formation temperature distribution characteristics in the Tarim Basin with depths of 1,000–5,000 m were partially affected by basement relief. In this study, the relatively low formation temperatures at depths of 6,000–10,000 m in the Awati Depression, northern Shuntuoguole Low-Uplift and Manjiaer Depression are probably related to deep basement positioning, while the relatively high formation temperature in the Central Uplift results from shallow basement positioning. Note that for the 1D steady-state heat transfer, the rock heat production rate and thermal conductivity are assumed to change with the depth (vertical direction); however, it should be noted that these processes also involve a lateral change of the thermal refraction effect between depression and uplift regions. Some studies utilize two-dimensional (2D) heat transfer simulations to better account for how basement relief affects the deep geothermal field of sedimentary basins

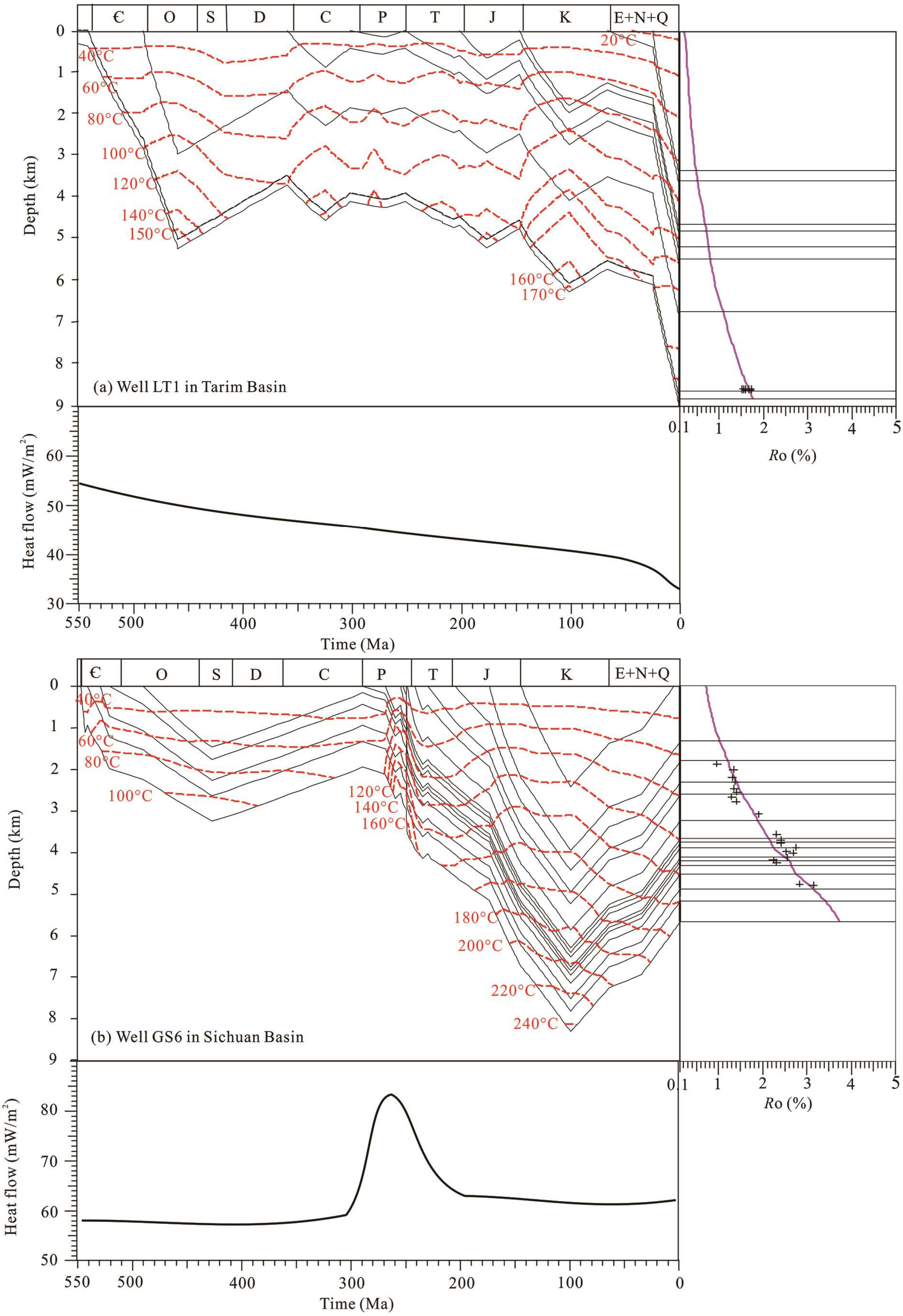

Fig. 6. Burial and thermal histories for well LT1 in the Tarim Basin and Well GS6 in the Sichuan Basin.

(Xiong and Gao, 1982; Weir and Furlong, 1987). Therefore, it must be acknowledged that the ultra-deep temperature calculated by the 1D heat transfer formula is limited to reflecting the thermal effect of basement relief. In addition, rapid subsidence since the Neogene has formed 'thermal blanketing' at the subsurface in the Tabei Uplift and the western Southwest Depression (Wangen, 1995; Qiu et al., 2012; Li et al., 2014; He, 2020),

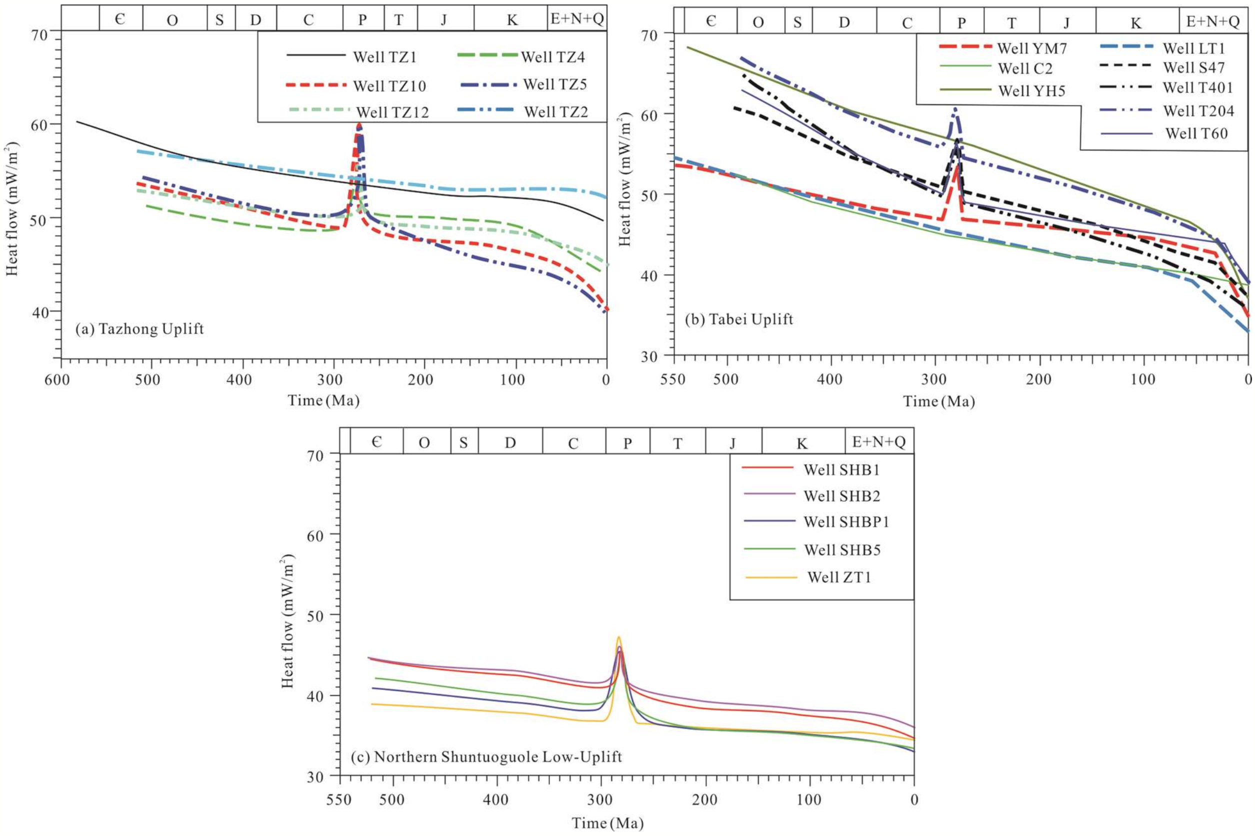

Fig. 7. The heat flow histories of the Tazhong Uplift, the Tabei Uplift and the northern Shuntuoguole Low-Uplift (Li et al., 2022) in the interior of the Tarim Basin.

reflecting the low heat flow and formation temperatures of these areas. Except for the basement relief, the highest heat flow and formation temperatures in the southeastern Tarim Basin are also related to the smallest thickness of thermal lithosphere at just ~130 km compared to other tectonic units (Fig. 9b, Chang et al., 2017a), which is related to the northward subduction of the Tibetan Plateau during the late Cenozoic.

Fault activity, especially for thrust faults and strike-slip faults, generates thermal anomalies through friction and heat convection (Barr and Dahlen, 1989; Wang et al., 2003; Liu and Zhang, 2011; McQuarrie and Ehlers, 2017). According to numerical simulation, Liu and Zhang (2011) suggested that the fault activity in the Bachu Uplift could lead the formation temperature near the faults to increase by up to ~12°C, and the temperature increment is decreased as the distance from the faults is increased. In the Kuqa Depression, the present-day heat flow and geothermal gradient decrease from north to south. Wang et al. (2003) considered that this resulted from friction heat and local heat convection due to late Cenozoic thrusting. The thermal effect of the fault activity weakens from north to south; thus, the northern Kuqa Depression shows a relatively higher thermal regime today (Figs. 2–4). Baietto et al. (2008) discussed the thermal effect of strike-slip faults in the regional geothermal field in the western Alps, explaining that when deeper heat is transmitted to shallow regions by the strike-slip faults, there can be an abnormal temperature increase along the two sides of the strike-slip faults. However, the effect time needed for this phenomenon to develop is relatively short, being several tens of thousands of years. In this case, the Shuntuoguole Low-Uplift developed many strike-slip faults striking NE, which occurred during the Paleozoic and late Cenozoic and served as channels for hydrocarbon migration from the deeper Yuertusi source rocks to the shallow Middle Ordovician reservoirs (Deng et al., 2018, 2019; Han, 2018). Therefore, we speculate that the past and deep geothermal fields in the Shunbei area were also affected by hydrocarbon migration. However, there is no evidence to show that the formation temperature near the strike-slip faults is different from other areas in the Shuntuoguole Low-Uplift (Liu et al., 2020; Li et al., 2022), implying that the thermal effect duration of the strike-slip faults is limited.

Thermal refraction generated by the contrast in thermal conductivity between salt and sediment usually results in a higher temperature than background above the salt and a lower temperature than surroundings at the base of the salt (Corrigan and Sweat, 1995). Based on the numerical simulations, Liu et al. (2017) considered that the Paleogene gypsum and salt layers in the Kuqa Depression generated a higher temperature in the overlying sediments with an increment of 10–20°C and a lower temperature below the salt layer with a decrement of 4–8°C compared to the surrounding layers at the same depth (Fig. 9c). As shown in Fig. 1b, the middle Cambrian gypsum and salt layers distributed in the Central Tarim Basin do contribute

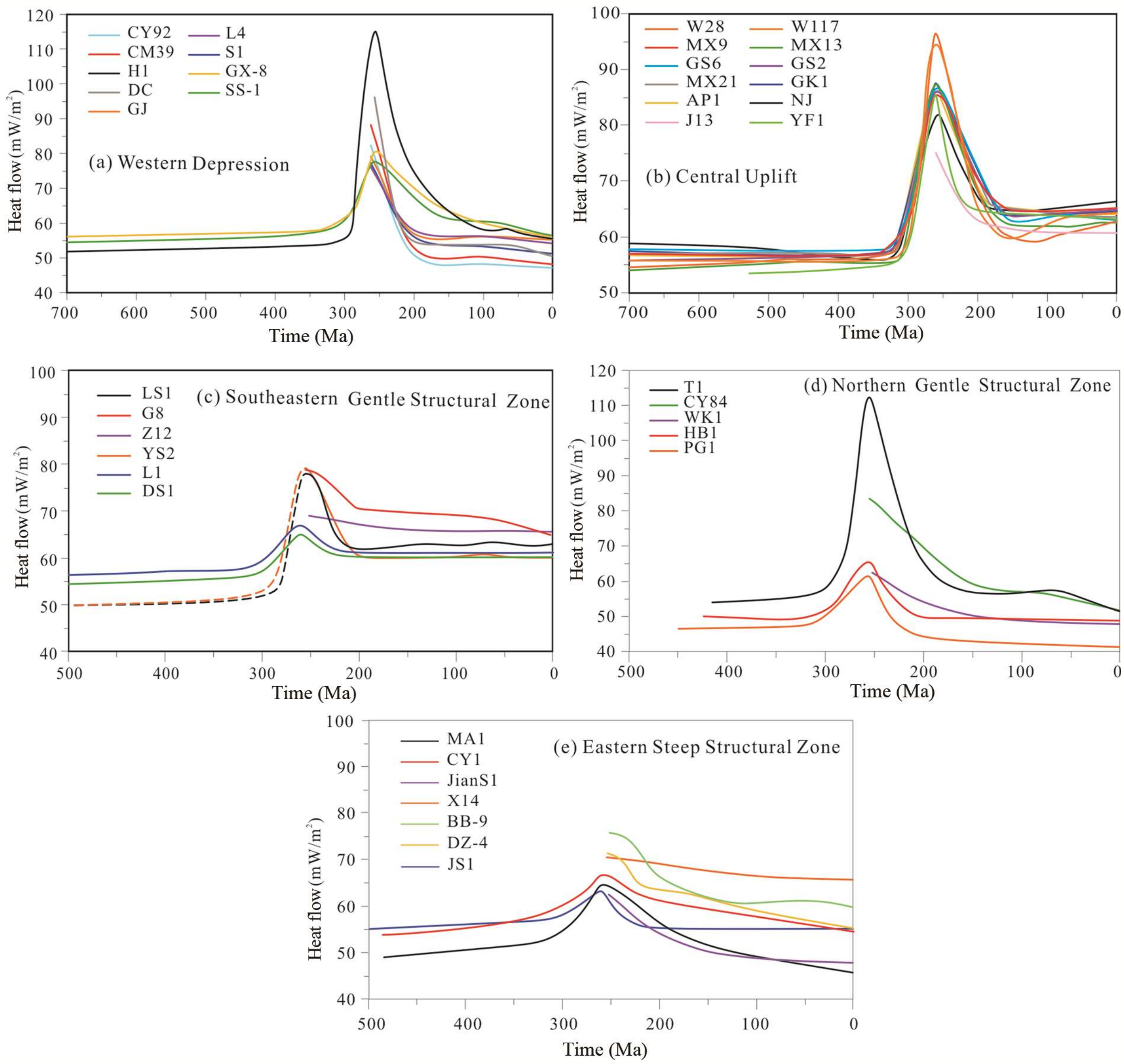

Fig. 8. Thermal histories of different tectonic units of the Sichuan Basin (Qiu et al., 2022).

to the makeup of the superdeep geothermal field. However, due to the large differences in the depths of these layers among the Bachu Uplift, Tazhong Uplift, Awati Depression and Shunbei Area, it is difficult to quantitatively evaluate this thermal effect to a certain depth. Liu et al. (2020) stated that hydrothermal upwelling in the southern Shuntuoguole Low-Uplift also contributes to a deeper high-temperature thermal anomaly with numerical modeling.

In addition, the different variation of the geothermal gradient with depth between the Tarim Basin and the Sichuan Basin is probably related to the rock heat production rate and thermal conductivity (Fig. 10). The rock heat production rate and thermal conductivity in the Sichuan Basin show no obvious correlation with the strata. In the Tarim Basin, the rock heat production rate and thermal conductivity gradually became larger and smaller, respectively, when the strata became older (implying that the formation depth increases). When the rock thermal conductivity becomes larger, the geothermal gradient would become smaller, as shown in Fig. 9a.

5.2 Maturation evolution of the lower Cambrian source rocks

Chang et al. (2022b) reported the temperature histories of the Yuertusi Formation source rock in the lower Cambrian of wells TS1 (Tabei Uplift) and SB5 (Shunbei Area) and the upper Cambrian of well ZS1 (Tazhong Uplift) (Fig. 11a), which indicated that these strata experienced a maximum temperature of 160–185°C because of rapid subsidence in the late Cenozoic. Such a high temperature can be thought to have resulted in gas generation and/or crude oil cracking. It is noteworthy that liquid hydrocarbons such as condensate oil and (volatile) light oil were found in the superdeep Cambrian or Ordovician strata in these three tectonic units (Yun and Zhai, 2008; Wang et al., 2014; Jiao, 2018). Previous studies illustrated that long-term high fluid pressure could inhibit the thermal evolution of source rocks (Hao et al., 1995; McTavish, 1998), in that the R_o under high fluid

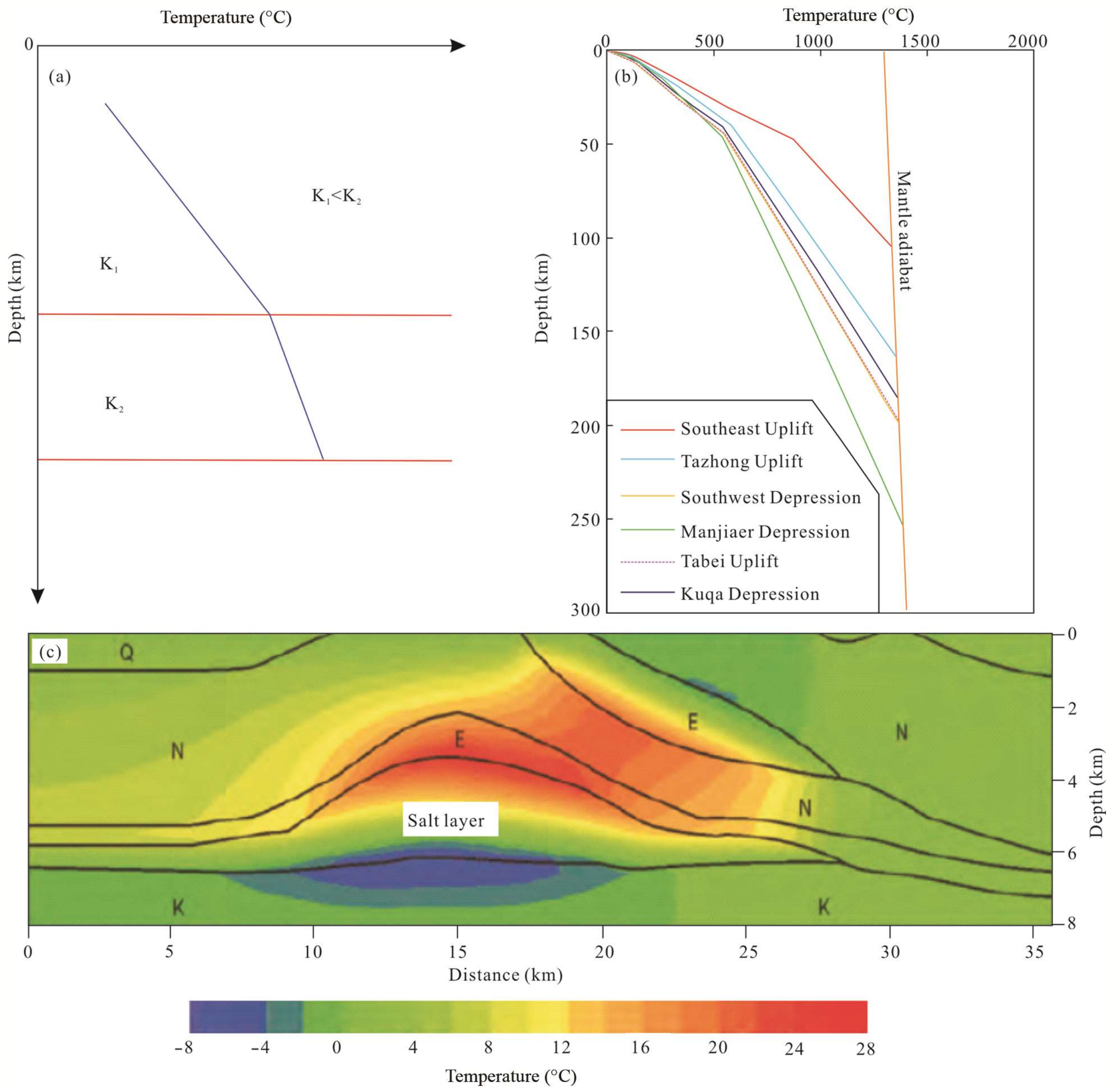

Fig. 9. (a) The temperature-depth polyline with the variation in the rock thermal conductivity; (b) calculated thermal lithosphere thickness of six tectonic units (Chang et al., 2017a); (c) abnormal temperature pattern related to the salt structure in the Kuqa Depression (Liu et al., 2017).

pressure could be ~0.5% lower than the normal value, which can prolong the generation time of liquid hydrocarbons. Although there is no evidence of abnormal overpressure in the Shunbei area, the fluid pressure is still high, due to the burial depth. The depth of the source rock in the Shunbei area has presently reached ~10,000 m with a high fluid pressure of ~100 MPa. Kinetic simulation of the hydrocarbon generation revealed that the Yuertusi source rock in the Shunbei area still has the potential to generate oil under relatively low temperature and high fluid pressure conditions (Fig. 11b). Thus, the superdeep formation in the Shunbei Area and the Tabei Uplift are potential areas for further petroleum exploration. The Qiongzhusi Formation source rock of the lower Cambrian in the whole Sichuan Basin experienced a maximum formation temperature greater than 220°C during the end of the Early Cretaceous (Fig. 12), which led the source rock to generate dry gas and crude oil cracking in the Lower Cambrian and Sinian reservoirs. As such, we are unable to discover oil fields in the deep Cambrian and Sinian strata for the Sichuan Basin today.

6 Conclusions

(1) The average heat flow and unified geothermal gradient indicate that the Tarim Basin and Sichuan Basin belong to the ‘cold’ and ‘warm’ basin types, respectively. The differential variation of the unified geothermal

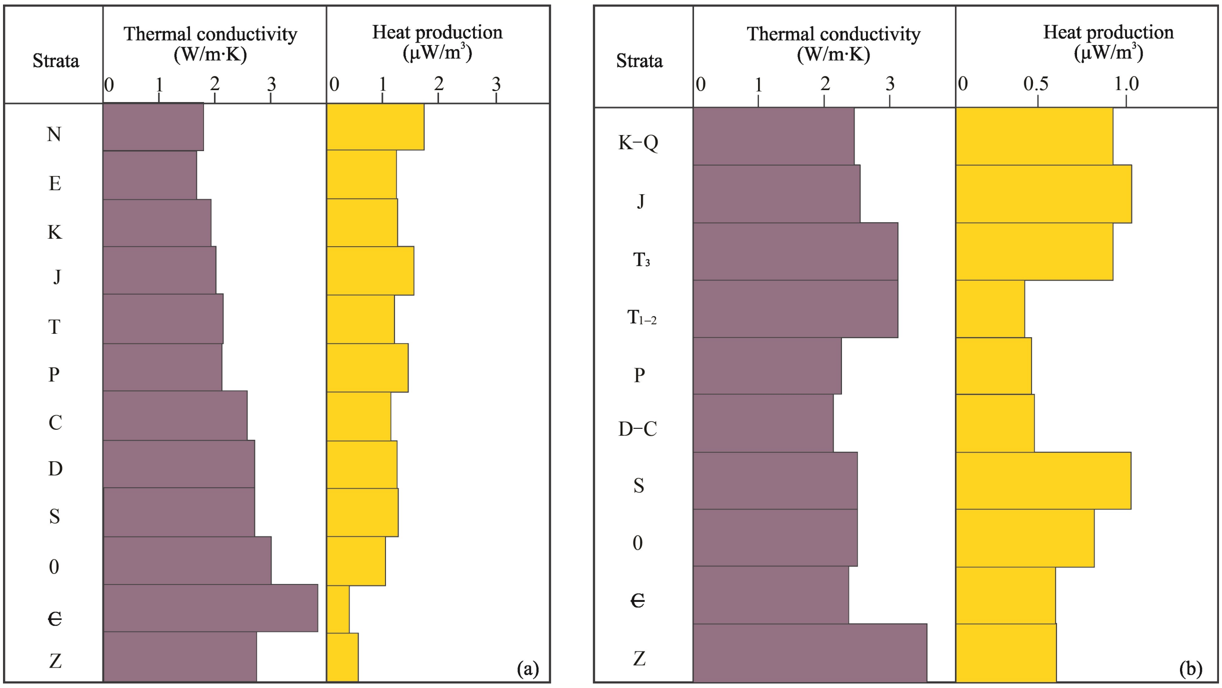

Fig. 10. Rock thermal conductivity and heat production rate data of the strata in the Tarim and Sichuan basins.

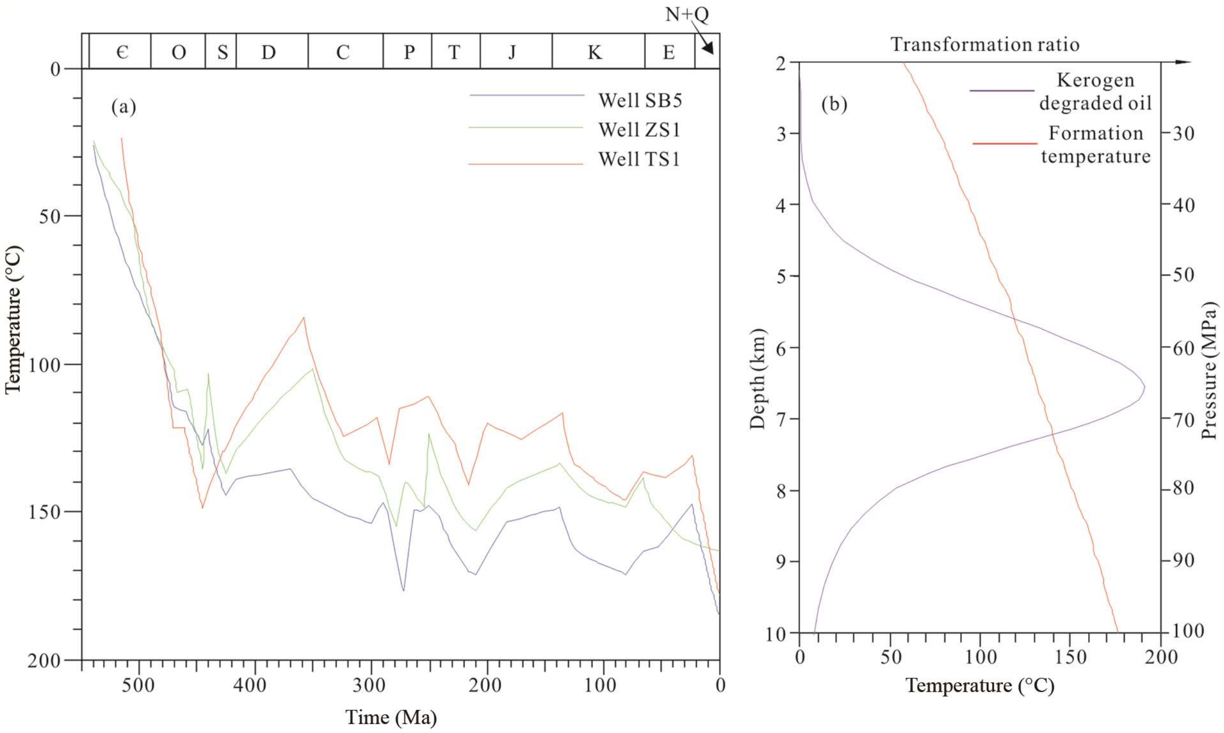

Fig. 11. (a) Temperature histories of the lower Cambrian in wells SB5 and ZS1 and the upper Cambrian in well TS1 (Chang et al., 2022b); (b) hydrocarbon generation kinetic simulation of the lower Cambrian source rock in well SB5.

gradient with depth between the Tarim and Sichuan basins is probably related to the diverse distribution of the rock heat production rate and thermal conductivity of the strata.

(2) This study calculated the formation temperatures with depths of 6,000–10,000 m in the Tarim Basin and 6,000–9,000 m in the Sichuan Basin. Their horizontal distribution was influenced by the basement relief, fault activity and hydrothermal upwelling.

(3) The paleo-heat flow of the Tarim Basin gradually decreased since the Early Cambrian, with an abrupt peak during the Early Permian, while that of the Sichuan Basin experienced three stages, including a stable state before

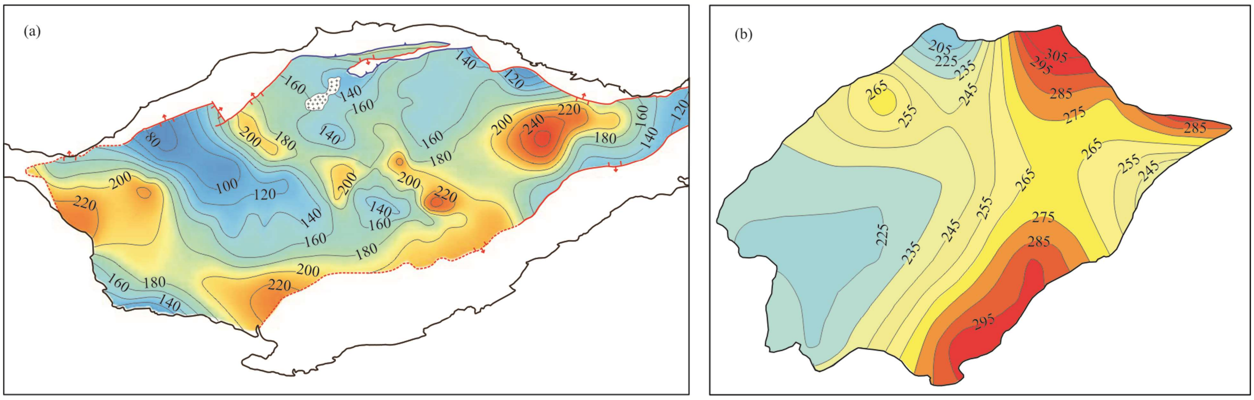

Fig. 12. (a) Present-day temperature distribution of the lower Cambrian Yuertusi Formation source rock in the Tarim Basin (Qiu et al., 2022); (b) late Early Cretaceous temperature distribution of the Lower Cambrian Qiongzhusi Formation source rock in the Sichuan Basin.

the Early Permian, rapid rise at the end of the Early Permian and a decline after the Late Permian.

(4) Due to the low thermal regime, the Lower Cambrian source rock in the interior of the Tarim Basin is suitable for liquid hydrocarbon generation, while the deep and ancient strata in the Sichuan Basin only retained natural gas in the background of a high thermal regime.

Acknowledgments

This work was supported by the National Key Research and Development Program of China (No. 2017YFC0603102) and the National Natural Science Foundation of China (No. U19B6003 and 41972125).

Manuscript received Feb. 25, 2022
accepted May. 31, 2022
associate EIC: ZHANG Shuichang
edited by Jeffery J. LISTON and FEI Hongcai

References

Baietto, A., Cadoppi, P., Martinotti, G., Perello, P., Perrochet, P., and Vuataz, F.D., 2008. Assessment of thermal circulations in strike-slip fault systems: the Terme di Valdieri case (Italian western Alps). Geological Society, London, Special Publications, 299(1): 317–339.

Barr, T.D., and Dahlen, F.A., 1989. Brittle frictional mountain building: 2. Thermal structure and heat budget. Journal of Geophysical Research, 94: 3923–3947.

Chang, J., Qiu, N., and Li, J., 2012. U-Pb dating of detrital zircon from the lower Silurian in the Keping Area of the Tarim Basin and its geological implications. Journal of Earth Sciences and Environment. 34(3): 22–33 (in Chinese with English abstract).

Chang, J., Qiu, N., Zhao, X., Xu, W., Xu, Q., Jin, F., Han C., Ma X., Dong X., and Liang, X., 2016a. Present-day geothermal regime of the Jizhong depression in Bohai Bay basin, East China. Chinese Journal of Geophysics-Chinese Edition, 59(3): 1003–1016 (in Chinese with English abstract).

Chang, J., Qiu, N.S., and Xu, W., 2017a. Thermal regime of the Tarim Basin, Northwest China: a review. International Geology Review, 59(1): 45–61.

Chang, J., Qiu, N.S., Li, C.X., Zhang, J.Y., Li, W.Z., and Fu, X.D., 2022a. Zircon He diffusion kinetics models and its implications on thermal history reconstruction of ancient strata in craton basins. China Journal of Geophysics-Chinese Edition, 65(2): 711–725 (in Chinese with English abstract).

Chang, J., Qiu, N.S., Song, X.Y., and Li, H.L., 2016b. Multiple cooling episodes in Central Tarim (Northwest China) revealed by apatite fission track analysis and vitrinite reflectance data. International Journal of Earth Sciences, 105(4): 1257–1272.

Chang, J., Qiu, N.S., Zhao, X.Z., Shen, F.Y., Liu, N., and Xu, W., 2018. Mesozoic and Cenozoic tectono-thermal reconstruction of the western Bohai Bay Basin (East China) with implications for hydrocarbon generation and migration. Journal of Asian Earth Sciences, 160: 380–395.

Chang, J., Tian, Y.T., and Qiu, N.S., 2017b. Mid-Late Miocene deformation of the northern Kuqa fold-and-thrust belt (southern Chinese Tian Shan): An apatite (U-Th-Sm)/He study. Tectonophysics, 694: 101–113.

Chang, J., Yang, X., Qiu, N.S., Min, K., Li, C.X., Li, H., and Li, D., 2022b. Zircon (U-Th)/He thermochronology and thermal evolution of the Tarim Basin, Western China. Journal of Asian Earth Sciences, 230, 105210.

Corrigan, J., and Sweat, M., 1995. Heat flow and gravity responses over salt bodies: a comparative model analysis. Geophysics, 60(4): 1029–1037.

Deng S., Li H., Zhang Z., Wu X., and Zhang J., 2018. Characteristics of differential activities in major strike-slip fault zones and their control on hydrocarbon enrichment in the Shunbei area and its surroundings, Tarim Basin. Oil & Gas Geology, 39(5): 878–888 (in Chinese with English abstract).

Deng, S., Li, H., Zhang, Z., Zhang, J., and Yang, X., 2019. Structural characterization of intracratonic strike-slip faults in the central Tarim Basin. AAPG Bulletin, 103(1): 109–137.

Feng, C., Liu, S., Wang, L. and Li, C., 2009. Present-day geothermal regime in Tarim Basin, northwest China. Chinese Journal of Geophysics, 52(11): 2752–2762 (in Chinese with English abstract).

Förster, A., Merriam, D.F., and Davis, J.C., 1997. Spatial analysis of temperature (BHT/DST) data and consequences for heat-flow determination in sedimentary basins. Geologische Rundschau, 86: 252–261.

Han, X., 2018. Formation and evolution of strike-slip faults in the Northern Slope of Tazhong Uplift, Tarim Basin. Beijing: Chinese University of Petroleum-Beijing (Ph. D. thesis): 1–133 (in Chinese).

Hao, F., Sun, Y.C., Li, S.T., and Zhang, Q.M., 1995. Overpressure retardation of organic-matter maturation and petroleum generation: A case study from the Yinggehai and Qiongdongnan basins, South China Sea. AAPG Bulletin. 79: 551–562.

He, D., Jia, C., Li, D., Zhang, C., Meng, Q., and Shi, X., 2005. Formation and evolution of polycyclic superimposed Tarim Basin. Oil & Gas Geology, 26: 64–77 (in Chinese with English abstracts).

He, D.F., Li, Y.Q., Huang, H.Y., Zhang, J., Lu, R.Q., and Li, D., 2020. Formation and hydrocarbon accumulation of the polycyclic and superimposed Sichuan Basin. Beijing: Science Press, 1–32 (in Chinese).

He, L., 2020. Thermal evolution of the Upper Yangtze Craton: Secular cooling and short-lived thermal perturbations. Physics

of the Earth and Planetary Interiors, 301: 106458.
Jia, C., 1997. Tectonic characteristics of the Tarim Basin in China and its oil-gas resources: Beijing: Petroleum Industry Press,1–8 (in Chinese).
Jiang, Q., Qiu, N., and Zhu, C., 2018. Heat flow study of the Emeishan large igneous province region: Implications for the geodynamics of the Emeishan mantle plume. Tectonophysics, 724–725: 11–27.
Jiao, F., 2018. Significance and prospect of ultra-deep carbonate fault-karst reservoirs in the Shunbei Area, Tarim Basin. Oil & Gas Geology, 39(2): 207–216 (in Chinese with English abstract).
Jin, Z.J., 2011. Formation and accumulation of oil and gas in marine carbonate strata in Chinese sedimentary basins. Science China Earth Science, 41(7): 910–926.
Li, D., Chang, J., Qiu, N., Wang, J., Zhang, M., Wu, X., Han, J., Li, H., and Ma, A., 2022. The thermal histories in sedimentary basins: a case study of the central Tarim Basin, Western China. Journal of Asian Earth Sciences, 229: 105149.
Li, J., Zhou, X., Li, W., Wang, H., Liu, Z., Zhang, H., and Ta, S., 2015. Preliminary reconstruction of tectonic paleogeography of Tarim Basin and its adjacent areas from Cambrian to Triassic, NW China. Geological Review, 61(6): 1225–1234 (in Chinese with English abstract).
Li, M., Wang, T., Chen, J., He, F., Yun, L., Akbar, S., and Zhang, W., 2010. Paleo-heat flow evolution of the Tabei Uplift in Tarim Basin, northwest China. Journal of Asian Earth Sciences, 37(1): 52–66.
Li, W., Jiao, Y., Zuo, Y., Song, X., and Qiu, N., 2014. Effect of deposition rate on geothermal field in the Bozhong depression, Bohai Bay Basin. Chinese Journal of Geophysics, 57(5): 1568–1577 (in Chinese with English abstract).
Li, Y.Q., Li, Z.L., Sun, Y.L., Santosh, M., Langmuir, C.H., Chen, H.L., Yang S.F., Chen, Z.X., and Yu, X., 2012. Platinum-group elements and geochemical characteristics of the Permian continental flood basalts in the Tarim Basin, northwest China: Implications for the evolution of the Tarim Large Igneous Province. Chemical Geology, 328: 278–289.
Li, Z.L., Chen, H.L., Song, B.A., Li, Y.Q., Yang, S.F., and Yu, X., 2011. Temporal evolution of the Permian large igneous province in Tarim Basin in northwestern China. Journal of Asian Earth Sciences, 42(5): 917–927.
Lin, C., Yang, H., Liu, J., Rui, Z., Cai, Z., and Zhu, Y., 2012. Distribution and erosion of the Paleozoic tectonic unconformities in the Tarim Basin, Northwest China: Significance for the evolution of paleo-uplifts and tectonic geography during deformation. Journal of Asian Earth Sciences, 46: 1–19.
Liu, B., and Zhang, J., 2011. The influence of geothermal evolution on the oil window of Bachu Uplift in Tarim Basin. Progress in Geophysics, 26(5): 1779–1787 (in Chinese with English abstract).
Liu, H., Wang, S., Cheng, B., Cao, Z., and Jiang, Z., 2021. Geochemical characteristics and migration pathways of Ordovician carbonate oil reservoirs in the Tuoputai area, Tarim Basin, northwestern China. Acta Geologica Sinica (English Edition), 95(4): 1295–1309.
Liu, S., Lei, X., Feng, C., and Hao, C., 2016. Estimation of subsurface formation temperature in the Tarim Basin, northwest China: implications for hydrocarbon generation and preservation. International Journal of Earth Sciences, 105: 1329–1351.
Liu, S., Yang, X., Qiu, N., Yang, S., and Li, X., 2017. Geothermal effects of salt structures on marine sedimentary basins and implications for hydrocarbon thermal evolution. Chinese Science Bulletin, 62: 1631–1644 (in Chinese with English abstract).
Liu, S., Yang, Y., Deng, B., Zhong, Y., Wen, L., Sun, W., Li, Z., Jansa, L., Li, J., Song, J., Zhang, X., and Peng, H., 2021. Tectonic evolution of the Sichuan Basin, Southwest China. Earth-Science Reviews, 213: 103470.
Liu, W., Qiu, N., Xu, Q., and Liu, Y., 2018. Precambrian temperature and pressure system of Gaoshiti-Moxi block in the central paleo-uplift of Sichuan Basin, southwest China. Precambrian Research, 313: 91–108.
Liu, Y., Qiu, N., Li, H., Ma, A., Chang, J., and Jia, J., 2020. Terrestrial heat flow and crustal thermal structure in the northern slope of Tazhong Uplift in Tarim Basin. Geothermics, 83: 101709.
Majorowicz, J., and Grasby, S.E., 2019. Deep geothermal energy in Canadian sedimentary basins vs. Fossils based energy we try to replace – Exergy [KJ/KG] compared. Renewable Energy, 141: 259–277.
McQuarrie, N., and Ehlers, T.A., 2017. Techniques for understanding fold-and-thrust belt kinematics and thermal evolution. In: Law, R.D., Thigpen, J.R., Merschat, A.J., and Stowell, H.H. (eds.), Linkages and Feedbacks in Orogenic Systems. GSA Memoir, 213: 25–54.
McTavish, R.A., 1998. The role of overpressure in the retardation of organic matter maturation. Journal of Petroleum Geology, 21: 153–186.
Poulsen, S.E., Balling, N., Bording, T.S., Mathiesen, A., and Nielsen, S.B., 2017. Inverse geothermal modelling applied to Danish sedimentary basins. Geophysical Journal International, 211(1): 188–206.
Putra, S., Suryantini, D.H., and Srigutomo, W., 2016. Thermal modeling and heat flow density interpretation of the onshore Northwest Java Basin, Indonesia. Geothermal Energy, 4(1): 12, doi:10.1186/s40517-016-0052-x.
Qiu, N., Chang, J., Zhu, C., Liu, W., Zuo, Y., Xu, W., and Li, D., 2022. Thermal regime of sedimentary basins in the Tarim, Upper Yangtze and North China Cratons, China. Earth-Science Reviews, 224: 103884.
Qiu, N., Chang, J., Zuo, Y., Wang, J., and Li, H., 2012. Thermal evolution and maturation of lower Paleozoic source rocks in the Tarim Basin, northwest China. AAPG Bulletin, 96(5): 789–821.
Sweeney, J.J., and Burnham, A.K., 1990. Evaluation of a simple model of vitrinite reflectance based on chemical kinetics. AAPG Bulletin, 74: 1559–1570.
Wang L., Li C., Liu S., Li H., Xu M., Wang Q., Ge R., Jia C., and Wei G., 2003. Geotemperature gradient distribution of Kuqa foreland basin, north of Tarim, China. Chinese Journal of Geophysics, 46(3): 403–407.
Wang, Z., Xie, H., Chen, Y., Qi Y., and Zhang, K., 2014. Discovery and exploration of Cambrian subsalt dolomite original hydrocarbon reservoir at Zhongshen-1 Well in Tarim Basin. China Petroleum Exploration, 19(2): 1–13 (in Chinese with English abstract).
Wangen, M., 1995. The blanketing effect in sedimentary basins. Basin Research, 7(4): 283–298.
Weir, L.A., and Furlong, K.P., 1987. Thermal regimes of small basins: Effects of intrabasinal conductive and advective heat transport. AAPG Memoir, 351–362.
Xiong, L.P., and Gao, W.A., 1982. Characteristics of geotherm in uplift and depression. Chinese Journal of Geophysics, 25 (5): 448–456 (in Chinese with English abstract).
Xu, M., Zhu, C.Q., Tian, Y.T., Rao, S., and Hu, H.B., 2011. Borehole temperature logging and characteristics of subsurface temperature in the Sichuan Basin. Chinese Journal of Geophysics, 54(4): 1052–1060 (in Chinese with English abstract).
Xu, Q., Qiu, N., Liu, W., Shen, A., and Wang, X., 2018. Thermal evolution and maturation of Sinian and Cambrian source rocks in the central Sichuan Basin, Southwest China. Journal of Asian Earth Sciences, 164: 143–158.
Xu, Y., Wei, X., Luo, Z., Liu, H., and Cao, J., 2014. The early Permian Tarim Large Igneous Province: Main characteristics and a plume incubation model. Lithos, 204: 20–35.
Yang, H., 2015. Exploration knowledge and direction of lower Proterozoic inner dolostones, Tarim Basin. Natural Gas Geoscience, 26(7): 1213–1223 (in Chinese with English abstract).
Yang, K., Zhang, B., Wang, X., He, L., Yang, H., Wang, P., Tang, J., Deng, J., and Zhang, C., 2020. Relationship between electrical properties and sedimentary environment of the Longmaxi Formation shale, southern Sichuan. Acta Geologica Sinica (English Edition), 94(5): 1531–1546.
Yang, X., Li, H., Yue, Y., Liu, S., Li, J., and Xiong, P., 2017. The strata and paleo-geomorphology framework at the end of

the Neoproterozoic and the development mode of source rocks at the beginning of the Cambrian. Natural Gas Geoscience, 28 (2): 189–198 (in Chinese with English abstract).
Yun, J., Jin, Z., and Xie, G., 2014. Distribution of major hydrocarbon source rocks in the lower Paleozoic, Tarim Basin. Oil & Gas Geology, 35(6): 827–838 (in Chinese with English abstract).
Yun, L., and Zhai, X., 2008. Discussion on characteristics of the Cambrian reservoirs and hydrocarbon accumulation in Well Tashen-1, Tarim Basin. Oil & Gas Geology, 29(6): 726–732 (in Chinese with English abstract).
Zhang, C., Zou, H., Li, H., and Wang, H., 2013. Tectonic framework and evolution of the Tarim Block in NW China. Gondwana Research, 23(4): 1306–1315.
Zhang, G., 2000. The formation and evolution of the Tarim cratonic basin in the Paleozoic and its hydrocarbons. Beijing: Geological Publishing House, 1–240 (in Chinese).
Zhang, X., Tian, J., and Peng, J., 2008. The lithofacies-paleogeography and space-time evolution of the Silurian-Devonian in the Tarim Basin. Acta Sedimentologica Sinica, 26(5): 762–771 (in Chinese with English abstract).
Zhou, Q., Tian, H., Wang, Y., and Xiao, X., 2015. The generation and evolution characteristics of the lower Cambrian shale in the central Sichuan Paleo-uplift. Natural Gas Geoscience, 26(10): 1883–1892 (in Chinese with English abstract).
Zhu, C., Xu, T., Qiu, N., Chen, T., Xu, M., and Ding, R., 2022. Distribution characteristics of the deep geothermal field in the Sichuan Basin and its main controlling factors. Frontiers in Earth Sciences, 10: 824056.
Zou, C., Du, J., Xu, C., Wang, Z., Zhang, B., Wei, G., Wang, T., Yao, G., Deng, S., Liu, J., Zhou, H., Xu, A., Yang, Z., Jiang, H., and Gu, Z., 2014. Formation, distribution, resource potential and discovery of the Sinian-Cambrian giant gas field, Sichuan Basin, SW China. Petroleum Exploration and Development, 41(3): 278–293 (in Chinese with English abstract).
Zou, C., Yang, Z., He, D., Wei, Y., Li, J., Jia, A., Chen, J., Zhao, Q., Li, Y., Li, J., and Yang, S., 2018. Theory, technology and prospects of conventional and unconventional natural gas. Petroleum Exploration and Development, 45(4): 575–587 (in Chinese with English abstract).
Zuo, Y., Jiang, S., Wu, S., Xu, W., Zhang, J., Feng, R., Yang, M., Zhou, Y., and Santosh, M., 2020. Terrestrial heat flow and lithospheric thermal structure in the Chagan Depression of the Yingen-Ejinaqi Basin, north central China. Basin Research, 32 (6): 1328–1346.

About the first and corresponding author

CHANG Jian, male, born in 1982 in Hengshui, Hebei Province; Professor of China University of Petroleum-Beijing. He is currently interested in the study of thermal histories of sedimentary basins and low temperature thermochronology. E-mail: changjian@cup.edu.cn.